# Virtual Code Resource Allocation Approach for Energy-Aware access of Machine-Type Communications over 5G Smart City

M. Condoluci[a], G. Araniti[a,*], M. Dohler[b], A. Iera[a], A. Molinaro[a]

[a] *University Mediterranea of Reggio Calabria, DIIES Department, Italy*
[b] *King's College London, Department of Informatics, UK*

**Abstract**

The enormous traffic of machine-type communications (MTC) expected over 5G smart city environments exacerbates the limitations of access schemes currently under investigation in literature. This becomes more challenging when considering the heterogeneity in the level of residual battery energy of machines and dictates novel solutions aiming at drastically reducing the collision probability of devices with critical level of residual battery energy. In this paper, we propose a virtual code resource allocation (VCRA) approach which extends the code-expanded strategy to support high number of devices simultaneously accessing the system and the virtual resource allocation scheme to introduce energy-priority in the access procedure. The idea behind our proposal is the definition of different access levels that exploit disjoint sets of access codewords, properly tailored to guarantee high capacity for each access level. Simulation results testify the effectiveness of our scheme in terms of *(i)* reducing the collision probability of machines with limited battery capabilities also in scenario with very huge cell load and *(ii)* enhancing the efficiency with respect to legacy code-expanded strategy.

*Keywords:* MTC, M2M, RACH, 5G

## 1. Introduction

A field of particular attention for network providers is the development of effective *smart city* solutions allowing cities to become a new complex ecosystem with innovative applications [1, 2] by simultaneously supporting different traffic types with unique features over next-to-come fifth generation (5G) systems [3]. An example of smart city environment is depicted in Fig. 1.

In this scenario, an important role will be played by *machine-type communications (MTC)*, which represent a novel transmission paradigm where machines (such as smart meters, cameras, remote sensors) send data without (or with minimal) human intervention [4]. In addition to smart city, MTC are expected to offer unprecedented opportunities and business models to telco operators in different fields (e.g., transport and logistics, smart power grids, e-health, home and/or remote surveillance) [5] and, consequently, have promising economic and strategic value for 5G wireless networks.

The effective management of MTC opens different research topics, such as ad-hoc cellular-compliant network architecture [6] and data transmission procedures, currently under investigation by industries and standardization bodies [7, 8]. In particular, being battery-constrained devices, machines aim to send data as quicker as possible to save battery and this dictates for the definition of an adequate access scheme [9] able to support the very high number of MTC devices expected over 5G networks [10]. Furthermore, the expected huge load of MTC devices has to be properly managed to avoid a negative impact of the performance of human traffic [11].

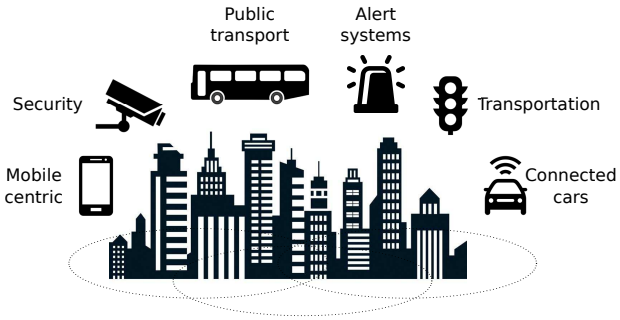


Figure 1: Example of application scenarios for 5G smart city.

The 3rd Generation Partnership Project (3GPP) standardized the contention-based random access channel (RACH) mechanism [12], where devices waits for a random access (RA) slot to send a randomly chosen orthogonal preamble: if two (or more) devices select the same preamble, a collision occurs and preamble transmission has to be re-accomplished. Due to the limited set of available preambles, the 3GPP RACH suffers in terms of *capacity* (i.e., the number of limited available preambles and, thus, associated access codewords) when the

*Corresponding author. University Mediterranea of Reggio Calabria, DIIES Department, 89124 Reggio Calabria, Italy. Email: araniti@unirc.it. Telephone and fax: +39 0965 1693420

*Email addresses:* massimo.condoluci@unirc.it (M. Condoluci), araniti@unirc.it (G. Araniti), mischa.dohler@kcl.ac.uk (M. Dohler), antonio.iera@unirc.it (A. Iera), antonella.molinaro@unirc.it (A. Molinaro)

number of devices accessing the network increases and this involves high delays and battery consumptions for both human and machine devices, as highlighted in [6]. Several works have been presented in literature aiming at overcoming the limitations of 3GPP RACH [9]. Among those, virtual resource allocation [13] and code-expanded strategies [14] have been designed to achieve access prioritization and higher capacity, respectively. The former approach deals with the separation of RA resources (i.e., preambles) into different sets to guarantee access separation for devices with different priorities while the latter foresees with a logical extension of the access method where devices send multiple preambles over multiple RA slots. Nevertheless, two main drawbacks can be associated to these schemes. The virtual resource allocation may require a high ratio of preambles for high-priority level(s) to guarantee low collision probability; this obviously may jeopardize the number of preambles for low-priority level(s) with thus performance degradation. The code-expanded approach introduces a novel issue known as phantom codes: since the access codeword is composed of multiple preambles, the base station hears different preambles in each RA slot and, consequently, the number of codewords computed by the base station (referred in the paper as 'decoded codewords') is basically the combination of preambles received in each slot. This means that the number of decoded codewords is higher than the number of codewords effectively transmitted by devices. This involves inefficiencies due to the fact that the management of phantom codes (i.e., codes not transmitted by accessing devices) requires a large amount of resources by the base station and this, consequently, increases the delay for RA procedure.

In this paper, we deal with an aspect not adequately investigated in literature, i.e., the design of an energy-aware access scheme. As also highlighted in [3, 7, 9], the set of machines accessing 5G systems is expected to be heterogeneous, where heterogeneity is also intended in terms of different levels of residual battery energy. In this direction, special care has to be reserved for devices with limited battery capabilities for which RACH collisions will involve a consumption of the already drastically low battery energy. By extending the virtual resource allocation and code-expanded approaches, the idea behind our proposal is to define different energy-based access levels and to split the set of available preambles into different subsets, each one associated to one access level. So doing, we can set the number of access levels as well as the number of associated codewords according to the measured cell load and the expected levels of residual battery energy. Our approach, namely *virtual code resource allocation (VCRA)*, outperforms the ones in literature by guaranteeing a different collision probability for each access level, with particular attention to devices with critical residual energy. With respect to 3GPP and the virtual resource allocation schemes, our proposed strategy increases the access capacity and consequently avoids human traffic degradation caused by MTC. With respect to legacy code-expanded, the use of different sets of access codewords at the basis of our approach reduces the side effects (i.e., latency and resource consumption) of phantom codes.

The remainder of this paper is structured as follows. Sec. 2 illustrates the related work, while Sec. 3 depicts the considered system model and analyzes the approaches considered as benchmark. Sec. 4 presents our proposal, whose effectiveness is testified through simulation results in Sec. 5. Sec. 6 gives the conclusions of this work and discusses about the future work.

## 2. Related Work

The design of an access procedure able to support the simultaneous access of both human- and machine-type devices is currently considered as one of the most challenging in the field of 5G smart city [9]. In this scenario, the reference scheme is represented by the 3GPP RACH [12], a contention-based RA mechanism which consists of a four-message handshake between the accessing devices and the base station. The RA procedure is performed in the following situations:

- Upon *initial access* to the network.
- For the reception/transmission of new data in case the device is *not synchronized*.
- Upon transmission of new data in case of *no scheduling request resources* are configured on the uplink control channel.
- During *handover* (i.e., change of associated BS) to avoid a session drop.
- For *connection re-establishment* after a radio link failure.

The steps of 3GPP RACH are depicted in Fig. 2. The contention-based 3GPP RACH procedure starts with the transmission of a preamble (Msg1) on the Physical Random Access Channel (PRACH). The PRACH is a periodic sequence of reserved uplink time-frequency resources (a.k.a. RA slots) whose periodicity is broadcasted by the BS in the PRACH Configuration Index. The amount of RA resources is thus given by two aspects: *(i)* the number of available preambles; *(ii)* the number of available RA slots. The preamble is randomly chosen among a predefined set of orthogonal pseudo-random preambles. A collision occurs if two or more devices transmit the same preamble in the same RA slot. If Msg1 is successfully decoded, the BS sends the Random Access Response (RAR, a.k.a. Msg2); the RAR[1] contains information about the detected preamble, uplink timing alignment, and the grant for the transmission of the Connection Request (Msg3) on the Physical Uplink Shared Channel (PUSCH). An undetected collision of preambles could also involve a Msg3 collision. The Msg3 also lists the device identifier and the buffer state report useful to the BS for scheduling the following data transmission. Finally, a Contention Resolution message (Msg4) terminates the RA procedure and confirms the grant for the subsequent data transmission on PUSCH.

[1]To reduce the overhead, the number of devices which can be included in each RAR message is limited according to the network providers settings. For instance, 3GPP considers that up to 6 devices can be simultaneously included within a single one RAR.

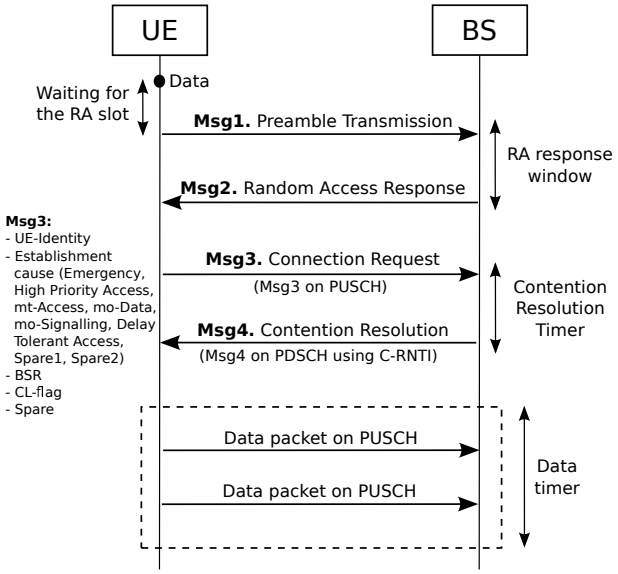


Figure 2: Time diagram of the 3GPP RACH.

The contention-based 3GPP-RACH is an *ALOHA-based* radio access, where devices start the access procedure in the first available opportunity; this could involve performance degradations such as high probability of collision in the case of huge load of simultaneous access requests. Consequently, the main limitation of 3GPP RACH is related to its limited capacity that is not able to fulfill the requirement of simultaneously human and machine access. To better understand this aspect, 3GPP performed some studies on the capacity limitations of the LTE RACH [15]. By considering that RA slots are available every 5ms and 54 preambles are used for contention-based access, the system offers 200 access opportunities per second, i.e., a capacity of about 11k preambles per second. By the way, it is worth noting that this number represents the absolute maximum capacity, i.e., the capacity in case of absence of collisions; in real scenarios, the effective capacity is severely reduced. Furthermore, it is also worth mentioning that preamble collisions require that colliding devices perform a novel RACH procedure and this involves additional access delays (which may involve QoS degradations for human-related smart city applications) and, consequently, battery consumption (which is mainly challenging for the lifetime of MTC devices). The latter aspect becomes more challenging when considering the presence of MTC devices with low level of residual battery. Indeed, for such devices, a Msg1 collision involves several preamble retransmission which may bring to consume the whole remaining battery charge. As a consequence, a RACH procedure properly designed to handle the heterogeneity access of devices in smart city environments has to manage *RA priority-differentiation* to guarantee, for instance, a lower collision probability to devices with limited battery capabilities.

Recent advances have been proposed to boost the performance of 3GPP RACH. A first enhancement is related to the *slotted access* approach which deals with the separation of RA slots for accessing devices [15]. This solution exploits dedicated RA slots for each terminal: the idea is that accessing devices calculate their corresponding RA slot (based, for instance, on their identity and additional parameters broadcasted by the BS) which is consequently exploited to start the RA procedure. The side effect of this approach is that, in order to allocate a dedicated RA slot per device in the case of huge load, larger RA cycles are needed thus drastically increasing the access delays. Following this direction, 3GPP [16] introduced the *Access Class Barring (ACB)* with the aim of enabling RA prioritization. In the case of network overload, the BS transmits a set of ACB parameters (in particular, a probability factor and the barring timer relevant to the pre-defined ACB classes) to differentiate among the accessing devices the RA slots used to transmit the preambles. According to ACB, accessing devices will draw a random number; if this number is lower than the probability factor, the device is able to attempt an access, otherwise, the access is barred and the device performs a random backoff time (according to the related barring timer value) before scheduling the preamble transmission. The ACB approach may guarantee short access delays to high-priority devices at the expense of a higher delay for other devices. It is worth noting that the introduced delay for low-priority devices may become really high because, in case of huge amount of devices, the Msg1 transmission is delayed for several RA slots.

Another interesting approach is the *virtual resource allocation* [13] which, with the aim of avoiding the negative impact that massive MTC may involve on human traffic, foresees to split the available RA resources into two subsets, one reserved for HTC and the other one for MTC devices. This purpose can be achieved by splitting the set of available preambles or by allocating different RA slots to HTC and MTC devices. By exploiting disjoint sets of preambles, the virtual resource allocation is able to guarantee RA differentiation as well as prioritization, for instance by dedicating a set of preambles to high-priority devices with critical level of residual battery. The main drawback is that, to guarantee very low collision probability for high-priority devices, high portion of preambles has to be reserved for these devices; consequently, the collision of other devices increases.

Finally, the *code-expanded* strategy [14] introduced the idea of transmitting multiple preambles in multiple RA slots instead of a single one preamble in only one RA slot. So doing, it is introduced the concept of *access codeword*, i.e., a sequence composed of different preambles. Due to the increased number of available access codewords, the use of code-expanded approach is suitable to effectively manage large number of devices which simultaneously perform the RA. Nevertheless, the use of multiple RA slots introduces a novel issue related to the phantom codes. If we suppose two devices whose access codewords are $\{A, B\}$ (i.e., the device sends the preamble $A$ in the first RA slot and the preamble $B$ in the second one, respectively) and $\{B, C\}$, then the base station hears the preambles $\{A, B\}$ in the first slot and the preambles $\{B, C\}$ in the second slot. This means that the base station decodes four different access codewords, i.e., $\{A, B\}$, $\{A, C\}$, $\{B, B\}$ and $\{B, C\}$, where two have been effectively transmitted by devices while remaining ones are the phantom codes. This aspect limits the efficiency of code-

expanded scheme since, due to the large number of decoded access codewords[2], the base station requires a large amount of time (i.e., time needed to send the following messages of RACH procedure) and resources (i.e., physical resources to send the Msg2 of RACH procedure, as well as the physical resources reserved for the transmission of related Msg3) to reply at each decoded codeword.

In this paper, we design a novel access strategy, namely *virtual code resource allocation (VCRA)*, which aims to overcome the limitations of above considered schemes. Our energy-aware scheme exploits the virtual resource allocation approach to guarantee RA prioritization by dividing available preambles into two disjoint sets: one is reserved for devices with low level of residual battery and one is exploited by remaining devices. Our proposal overcomes the capacity limitations of virtual resource allocation and legacy 3GPP RACH through the exploitation of the code-expanded strategy, which allows to increase the set of admissible access codewords thus limiting the negative impact of splitting the available preambles into two different subsets. Our approach has higher capacity (in terms of number of associated access codewords) compared to the 3GPP RACH while, compared to code-expanded, it offers higher efficiency (in terms of reduced number of phantom codes).

## 3. System model

We consider a device set $\mathcal{K} = \{1, 2, \ldots, K\}$; each device $k \in \mathcal{K}$ attempts to access a RA frame composed of $S$ different slots. Within each RA slot, a device randomly selects a preamble from the set $\mathcal{M} = \{1, 2, \ldots, M\}$ of available orthogonal preambles. So doing, the access codeword is composed from a sequence of $S$ orthogonal preambles (i.e., one preamble for each RA slot). According to $\mathcal{M}$ and $S$, a number equal to $A$ of different access codewords are available to be selected by accessing devices. We denote with $N_t$ the number of codewords decoded by the base station within one RA frame; such a number is the sum of three values: single codewords, denoted with $N_s$, i.e., the codewords used by single MTC device(s); colliding codewords, indicated with $N_c$; phantom codewords, denoted with $N_p$.

By assuming that the number of devices contending per codeword is modeled by a random variable $X$ [14], the probability of having $d$ devices contending for a given codeword in the same RA frame is given by:

$$\Pr[X = d] = \binom{K}{d}\left(\frac{1}{A}\right)^d\left(1 - \frac{1}{A}\right)^{K-d} \tag{1}$$

According to eq. (1), the expected number of single codewords can be computed as $N_s = A \cdot \Pr[X = 1]$, i.e.,:

$$N_s = A \cdot \binom{K}{1}\left(\frac{1}{A}\right)^1\left(1 - \frac{1}{A}\right)^{K-1} = K\left(1 - \frac{1}{A}\right)^{K-1} \tag{2}$$

Similarly, the expected number of colliding codewords is given by $N_c = A \cdot \Pr[X > 1] = A \cdot (\Pr[X = 0] - \Pr[X = 1])$, i.e.,:

$$N_c = A \cdot \left(1 - \left(1 - \frac{1}{A}\right)^K - \frac{K}{A}\left(1 - \frac{1}{A}\right)^{K-1}\right) \tag{3}$$

By considering the parameters defined above, we can compute two different parameters to measure the performance of random access policies. The first is the collision probability, which takes into account the fraction of colliding codewords and it is given by:

$$\rho = \frac{N_c}{N_t} \tag{4}$$

The second is the efficiency[3], designed as follows:

$$\eta = \frac{1}{2} \cdot \left[(1 - \rho) + \frac{N_s}{N_t}\right] \tag{5}$$

i.e., $\eta$ increases with higher values of success probability $(1-\rho)$ and the number $N_s$ of codewords received by the BS. Furthermore, it is worth noting that the efficiency is defined to take into account the overall number of decoded codewords received by the BS and, in particular, $\eta$ decreases in case of huge number of phantom codes.

### 3.1. 3GPP RACH

The 3GPP RACH [12] is based on the ideas of *(i)* sending only one preamble to the base station ($S$=1) and of *(ii)* exploiting the whole set of available preambles. Consequently, the set of access codewords is given by $A = M$; according to the $A$ value, the number of single and colliding codewords can be found as in (2) and (3), respectively.

A key aspect of 3GPP RACH is that the number $N_t$ of decoded codewords is equal to $N_t = N_s + N_c$; this means that $N_p = 0$. Indeed, the 3GPP RACH does not suffer in terms of phantom codes as the RA frame is composed of only one RA slot.

### 3.2. Virtual resource allocation

The virtual resource allocation (VRA) [13] extends the 3GPP RACH to guarantee priority-separation among accessing devices. The idea behind the VRA scheme is to split the set of available access preambles into different disjoint subsets, used for access differentiation purposes during the random access procedure. Let $L$ be the access levels and let $\mathcal{M}_l$ be the set of preambles associated to access level $l$, with $l = 1, \ldots, L$. We assume that $\cup_{l=1}^{L} \mathcal{M}_l = \mathcal{M}$, and that $\mathcal{M}_{l_1} \cap \mathcal{M}_{l_2} = \{\emptyset\}$, with $l_1, l_2 = 1, \ldots, L$ and $l_1 \neq l_2$. As a consequence, $A_l = |\mathcal{M}_l|$, and $\sum_{l=1}^{L} A_l = M$.

According to the VRA RACH, each device performs the access procedure by taking into account the associated access level. This means that the device set $\mathcal{K}$ is split into $L$ different subsets, denoted with $\mathcal{K}_l$ (where $l = 1, \ldots, L$). We assume

[2]With the term 'decoded codewords', we consider the access codewords computed by the base station according to preambles received within each RA slot. Decoded codewords are composed of single (i.e., non-colliding), colliding and phantom codewords.

[3]Similarly to [14], the approximation of evaluating the efficiency and the collision probability as the ratio of the expectations holds with the increase of the number of contending devices.

that $\cup_{l=1}^{L} \mathcal{K}_l = \mathcal{K}$, and that $\mathcal{K}_{l_1} \cap \mathcal{K}_{l_2} = \{\emptyset\}$, with $l_1, l_2 = 1, \ldots, L$ and $l_1 \neq l_2$. A generic device $k \in \mathcal{K}_l$ randomly selects one the preambles related to the respective access level, i.e., $\mathcal{M}_l$, to be transmitted in the RA slot. According to eq. (2) and ((3), the expected number of overall single codewords (i.e., considering all the access levels) can be computed as:

$$N_s = \sum_{l=1}^{L} \left( |\mathcal{K}_l| \left( 1 - \frac{1}{A_l} \right)^{|\mathcal{K}_l|-1} \right) \tag{6}$$

Similarly, the expected number of colliding codewords can be computed as follows:

$$N_c = \sum_{l=1}^{L} \left( A_l \cdot \left( 1 - \left( 1 - \frac{1}{A_l} \right)^{|\mathcal{K}_l|} - \frac{|\mathcal{K}_l|}{A_l} \left( 1 - \frac{1}{A_l} \right)^{|\mathcal{K}_l|-1} \right) \right) \tag{7}$$

Similarly to 3GPP RACH, the number $N_t$ of decoded codewords for the VRA RACH is equal to $N_t = N_s + N_c$, due to the fact that $S = 1$.

### *3.3. Code expanded RACH*

The code-expanded (CE) RACH [14] is based on the idea that the access procedure is performed on a RA frame-basis, instead of a RA slot-basis (i.e., $S > 1$). As a consequence, the access codeword is an access sequence composed of more than one preamble. In detail, the access codeword consists of a sequence composed of $S$ items, i.e., each device sends a preamble belonging to $\mathcal{M}$ within each RA slot of the frame. In this way, by considering the set $\mathcal{M}$ of admissible preambles plus the *idle* preamble which is used to model the case when the MTC devices do not transmit any preamble in the RA slot [14], the number of admissible access codewords is $A = (M+1)^S - 1$.

To compute the collision probability and the efficiency of CE RACH, it is necessary to compute the value of $N_t$ as the phantom codes decoded by the base station need to be properly evaluated. With this aim, the value of $N_t$ can be derived through a transition matrix $\mathbf{M}$, computed with an iterative approach composed by $S$ steps (please, refer to [14] for further details). The matrix related to the first step is equal to:

$$\mathbf{P}_1 = \begin{bmatrix} 1 & M & & & \\ & 2 & M-1 & & \\ & & \ddots & \ddots & \\ & & & M & 1 \\ & & & & M+1 \end{bmatrix} \tag{8}$$

At the $(s+1)$-th step (with $s = 1, \ldots, S-1$), the transition matrix is computed as follows:

$$\mathbf{P}_{s+1} = \begin{bmatrix} \mathbf{P}_s & M\mathbf{P}_s & & & \\ & 2\mathbf{P}_s & (M-1)\mathbf{P}_s & & \\ & & \ddots & \ddots & \\ & & & M\mathbf{P}_s & \mathbf{P}_s \\ & & & & (M+1)\mathbf{P}_s \end{bmatrix} \tag{9}$$

Once the $S$ iterations are computed, these following steps need to be accomplished to obtain the final value of $\mathbf{P}_S$: *(i)* the first row and first column are deleted; *(ii)* all entries on the diagonal of the resulting matrix are decreased by one (since the all-idle codeword is no longer a valid choice); *(iii)* the transition matrix is normalized with $\frac{1}{(M+1)^S - 1}$. The row removed from the transition matrix represents the initial state vector, denoted with $\boldsymbol{\pi}^{(1)}$.

An iterative approach is also exploited to derive the cardinality state vector $\boldsymbol{\alpha}$ as follows:

$$\boldsymbol{\alpha}^{(1)} = \left[ 1, 2, \ldots, M+1 \right] \tag{10}$$

$$\boldsymbol{\alpha}^{(s+1)} = \left[ \boldsymbol{\alpha}^{(s)}, 2\boldsymbol{\alpha}^{(s)}, \ldots, (M+1)\boldsymbol{\alpha}^{(s)} \right] \tag{11}$$

Once the $S$ iterations are computed, the $\boldsymbol{\alpha}^{(S)}$ vector is obtained by the removing first entry of the state cardinality vector and by decreasing by one the other entries.

Finally, the value of $N_t$ can be obtained as follows:

$$N_t = \sum_{i=1}^{A} \alpha_i^{(S)} \pi_i^{(K)} \tag{12}$$

where

$$\boldsymbol{\pi}^{(K)} = \frac{1}{(M+1)^S - 1} \boldsymbol{\pi}^{(1)} \cdot \mathbf{P}_S^{K-1} \tag{13}$$

It is worth noting that, by exploiting this approach, the obtained value of $N_t$ takes into consideration the values of $N_s$ and $N_c$. Nevertheless, $N_s$ and $N_c$ can be achieved through (2) and (3), respectively, by considering the overall set of codewords to be composed by $A = (M+1)^S - 1$ items.

## 4. The Virtual Code Resource Allocation

Our proposed priority-based code-expanded access scheme extends the philosophy of VRA RACH by splitting the set of available access preambles into different disjoint subsets while simultaneously adopting a code-expanded approach to increase the set of available access codewords. We name our proposal as virtual code resource allocation (VCRA). Our strategy is characterized by $L$ access levels and by a RA frame composed by $S > 1$ slots. Similarly to VRA RACH, we define with $\mathcal{M}_l$ the set of preambles associated to access level $l$, with $l = 1, \ldots, L$. We assume that $\cup_{l=1}^{L} \mathcal{M}_l = \mathcal{M}$, and that $\mathcal{M}_{l_1} \cap \mathcal{M}_{l_2} = \{\emptyset\}$, with $l_1, l_2 = 1, \ldots, L$ and $l_1 \neq l_2$. For the access level $l$, the number of associated codewords is given by $A_l = |\mathcal{M}_l|^S$, i.e., our solution does not exploit idle preambles. The overall number of available codewords is thus given by $A = \sum_{l=1}^{L} A_l < M^S < (M+1)^S$. It emerges that splitting the available preambles into different sets decreases the overall number of access codewords; nevertheless, we will show the benefits introduced by this approach in guaranteeing differentiation in the collision probability of different access classes.

An example of codewords generated by our proposed VCRA approach is shown in Tab. 1. It is worth noting that our scheme does not consider the exploitation of idle preambles. Although this choice reduces the number of available codewords, it introduces an efficiency increase due to the reduction in the number

of phantom codes computed by the base station. This aspect will be clearly highlighted in the simulation results.

Table 1: Codebook, $S = 2, M = 5, L = 2$

| | $l = 1$ | | $l = 2$ | |
|---|---|---|---|---|
| | $\|\mathcal{M}_1\| = 2$ | | $\|\mathcal{M}_2\| = 3$ | |
| Codeword | $s = 1$ | $s = 2$ | $s = 1$ | $s = 2$ |
| 1 | A | A | C | C |
| 2 | A | B | C | D |
| 3 | B | A | C | E |
| 4 | B | B | D | C |
| 5 | - | | D | D |
| 6 | - | | D | E |
| 7 | - | | E | C |
| 8 | - | | E | D |
| 9 | - | | E | E |

Similarly to the VRA RACH, the expected number of overall single and colliding codewords (i.e., considering all the access levels) can be computed as (6) and (7), respectively. The only difference compared to VRA RACH is given to the fact to the codeword sets of our proposed scheme is higher compared to VRA RACH due to the fact that we exploit $S > 1$ (i.e., $A_l = |\mathcal{M}_l|^S > |\mathcal{M}_l|$).

Being based on a code-expanded approach, the calculation of $N_t$ requires to take into consideration the number of phantom codes decoded by the base station. This aspect will be discussed in the remainder of this Section.

### *4.1. Calculation of $N_t$*

By considering $L$ different access levels, the value $N_t$ is given by:

$$N_t = \sum_{l=1}^{L} N_{t,l} \tag{14}$$

where $N_{t,l}$ indicates the number of codewords perceived by the base station related to access level $l$.

The calculation of $N_{t,l}$ is based on a Markov Chain (MC)[4] that describes the evolution of the number of codewords by considering $|\mathcal{K}_l|$ devices contending for the access level $l$. We remark the assumption that devices select their codewords independently from the set of available codewords according to their respective access level.

The MC states are determined by considering the preambles observed by the base station in each frame; we denote with $C_{s,l}$ the number of preambles received by the base station in the $s$-th RA slot relevant to the access level $l$. By considering the example in Tab. 1, we can note that each codeword is thus associated to the state (1,1), as each codeword is related to the transmission of only one preamble in each RA slot. According to the values of $C_{s,l}$, we can compute the cardinality $\alpha_{i,l}$ of the $i$-th state as the overall number of codewords decoded by the base station; this value is given by:

$$\alpha_{i,l} = \sum_{l=1}^{L} \left( \prod_{s=1}^{S} C_{s,l} \right) \tag{15}$$

By extending the approach in [14], the value of $N_{t,l}$ can be recast as the as ratio of the average cardinality of the set of the codewords perceived over the probability distribution of the MC states after $|\mathcal{K}_l| - 1$ transitions.

We now consider an example on the derivation of $N_{t,l}$ for the example related to the codebook listed in Tab. 1. By focusing, for instance, on the access level $l = 2$, we have that $|\mathcal{M}_2| = 3$. Consequently, $A_2 = 9$, the MC is characterized by 9 different states as shown in Tab. 2. The transitions among the states with the related probabilities are depicted in Fig. 3.

Table 2: Transition states for $S = 2, |\mathcal{M}_l| = 3$

| State | $C_{1,l}$ | $C_{2,l}$ | $\alpha_{i,l}$ | Transitions |
|---|---|---|---|---|
| 1 | 1 | 1 | 1 | 1,2,4,5 |
| 2 | 1 | 2 | 2 | 2,3,5,6 |
| 3 | 1 | 3 | 3 | 3,6 |
| 4 | 2 | 1 | 2 | 4,5,7,8 |
| 5 | 2 | 2 | 4 | 5,6,8,9 |
| 6 | 2 | 3 | 6 | 6,9 |
| 7 | 3 | 1 | 3 | 7,8 |
| 8 | 3 | 2 | 6 | 8,9 |
| 9 | 3 | 3 | 9 | 9 |

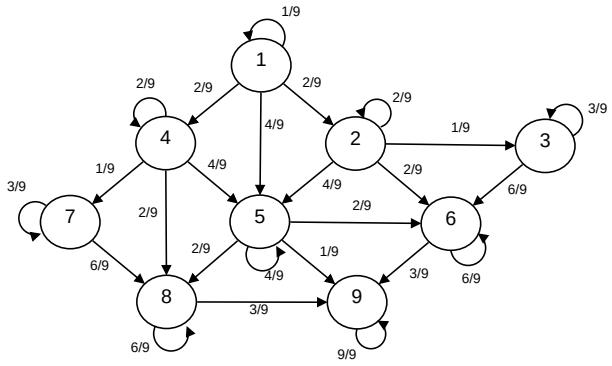


Figure 3: Example of Markov Chain for the example in Tab. 2.

The value of $N_{t,2}$ can be obtained trough an iterative method. If we consider only one device for the access level $l = 2$, the system can be only in state 1 (the same holds for the access level $l = 1$). As a consequence, the probability of the state being at state (1,1) when one device accesses the system is equal to 1, as all access codewords are related to the same state of the MC and no idle preambles are allowed. We can describe this situation through an initial state probability vector, denoted by $\boldsymbol{\pi}_2^{(1)}$, formed by $A_2 = 9$ items (i.e., one item for each state), where the first item is set to 1 while other items are equal to zero. The same reasoning holds the access level $l = 1$, the only difference is related to the different value of $A_1$. Therefore, when one de-

[4] A similar approach can be found in [14], although authors only described the case when idle preambles are allowed to devices. Differently, our proposal does not consider the exploitation of idle preambles; as remarked in the following, this modifies the analytical formulation compared to [14].

vice performs our proposed random access procedure ($|\mathcal{K}_l| = 1$ in the general case), the overall number of access codewords related to access level $l$ perceived by the base station is given by:

$$N_{t,l} = \sum_{i=1}^{A_l} \alpha_{i,l} \cdot \pi_l^{(1)} \tag{16}$$

Thus, by assuming $|\mathcal{K}_1 = 1|$ and $|\mathcal{K}_2 = 1|$, we obtain that $N_{t,1} = N_{t,2} = 1$.

When we consider a second device belonging to $l = 2$, the system can switch into states 1, 2, 4, or 5. If, for instance, we consider that the first user selected the codeword $(C, C)$, the system remains on the state (1,1) only if the second devices selects the same access codewords. If the second device selects one of the codewords $(C, D)$ or $(C, E)$, thus the system reaches the state (1,2), while the system is on state (2,1) if the second device selects the codeword $(D, C)$ or $(E, C)$. Finally, the system will be in state (2,2) if the second device chooses the codewords $(D, D)$, $(D, E)$, $(E, D)$, $(E, E)$. Consequently, the transition probability $\boldsymbol{P}_2$ (where 2 is related to the fact that we are focusing on the access level $l = 2$) is given by the ratio of the number of codewords that enable the transition and the total number of available codewords, i.e., in the considered example for $l = 2$:

$$\mathbf{P}_2 = \frac{1}{9}\begin{bmatrix} 1 & 2 & 0 & 2 & 4 & 0 & 0 & 0 & 0 \\ 0 & 2 & 1 & 0 & 4 & 2 & 0 & 0 & 0 \\ 0 & 0 & 3 & 0 & 0 & 6 & 0 & 0 & 0 \\ 0 & 0 & 0 & 2 & 4 & 0 & 1 & 2 & 0 \\ 0 & 0 & 0 & 0 & 4 & 2 & 0 & 2 & 1 \\ 0 & 0 & 0 & 0 & 0 & 6 & 0 & 0 & 3 \\ 0 & 0 & 0 & 0 & 0 & 0 & 3 & 6 & 0 \\ 0 & 0 & 0 & 0 & 0 & 0 & 0 & 6 & 3 \\ 0 & 0 & 0 & 0 & 0 & 0 & 0 & 0 & 9 \end{bmatrix}$$

where the entry $(i, j)$ is the transition probability that the system switch from state $i$ to state $j$.

#### 4.1.1. Derivation of $\boldsymbol{P}_l$ in the general case

By focusing on a generic access level $l$, the related transition matrix $\boldsymbol{P}_l$ is constructed with an iterative approach composed of $S$ steps. In the first step, the matrix $\boldsymbol{P}_{l,1}$ is given by:

$$\boldsymbol{P}_{l,1} = \begin{bmatrix} 1 & |\mathcal{M}_l| - 1 & & & & \\ & 2 & |\mathcal{M}_l| - 2 & & & \\ & & \ddots & \ddots & & \\ & & & |\mathcal{M}_l| - 1 & 1 & \\ & & & & & |\mathcal{M}_l| \end{bmatrix} \tag{17}$$

At the step $s + 1$, with $s = 1, \ldots, S - 1$, the transition matrix is given by:

$$\mathbf{P}_{l,s+1} = \begin{bmatrix} \mathbf{P}_{l,s} & (|\mathcal{M}_l| - 1)\mathbf{P}_{l,s} & & & \\ & 2\mathbf{P}_{l,s} & (|\mathcal{M}_l| - 2)\mathbf{P}_{l,s} & & \\ & & \ddots & \ddots & \\ & & & (|\mathcal{M}_l| - 1)\mathbf{P}_{l,s} & \mathbf{P}_{l,s} \\ & & & & |\mathcal{M}_l|\mathbf{P}_{l,s} \end{bmatrix} \tag{18}$$

Finally, the transition matrix is then achieved as $\boldsymbol{P}_l = \frac{1}{A_l}\boldsymbol{P}_{l,S}$.

#### 4.1.2. Derivation of $\boldsymbol{\pi}_l$ in the general case

The initial state vector $\boldsymbol{\pi}_l^{(1)}$ is composed by $|\mathcal{M}|_l$ items, where the first item is set to 1 and other ones are equal to zero, i.e.,:

$$\boldsymbol{\pi}_l^{(1)} = \frac{1}{|\mathcal{M}_l|}\begin{bmatrix} |\mathcal{M}_l| & 0 & \cdots & 0 \end{bmatrix} \tag{19}$$

By considering $|\mathcal{K}|_l$ devices accessing in the same RA frame, the state probability distribution $\pi_l^{(|\mathcal{K}|_l)}$ can be computed as:

$$\boldsymbol{\pi}_l^{(|\mathcal{K}|_l)} = \boldsymbol{\pi}_l^{(1)} \cdot \boldsymbol{P}_l^{|\mathcal{K}|_l - 1} \tag{20}$$

#### 4.1.3. Derivation of $\boldsymbol{\alpha}_l$ in the general case

Similarly to $\boldsymbol{P}_l$, the cardinality state vector $\boldsymbol{\alpha}_l$ can be obtained with $S$ different iterations. At the first iteration, the vector $\boldsymbol{\alpha}_l^{(1)}$ is equal to:

$$\boldsymbol{\alpha}_l^{(1)} = \begin{bmatrix} 1 & 2 & \cdots & |\mathcal{M}_l| \end{bmatrix} \tag{21}$$

At the step $s + 1$, with $s = 1, \ldots, S - 1$, the cardinality state vector is given by:

$$\boldsymbol{\alpha}_l^{(s+1)} = \begin{bmatrix} \boldsymbol{\alpha}_l^{(s)} & 2\boldsymbol{\alpha}_l^{(s)} & \cdots & |\mathcal{M}_l|\boldsymbol{\alpha}_l^{(s)} \end{bmatrix} \tag{22}$$

#### 4.1.4. Derivation of $N_{t,l}$ in the general case

The value of $N_{t,l}$ can be finally obtained as follows:

$$N_{t,l} = \sum_{l=1}^{A_l} \alpha_{l,i} \cdot \pi_{l,i}^{(|\mathcal{K}_l|)} \tag{23}$$

Once the values $N_{t,l}$ are obtained for all the access levels $l = 1, \ldots, L$, the overall value $N_t$ can be computed as in eq. (14). Finally, according to single and colliding codewords measured according to (6) and (7), respectively, the collision probability is measured as in (4) while the efficiency is measured as in (5).

## 5. Simulation Results

The effectiveness of our priority-based VCRA RACH strategy is assessed by comparing our proposed RA procedure with legacy 3GPP, VRA and CE schemes. We consider a simulation scenario based on physical settings of LTE systems [17]. To deal with simulative parameters widely exploited in literature, we use the settings in [9], where 54 preambles are dedicated to contention-based access (i.e., $M = 54$). We vary the load of devices which access the system in a time interval of $10ms$, and we consider a RACH periodicity of $5ms$ [9]. This implies that 3GPP and VRA schemes (where $S = 1$) have two different RA frames in the interval of $10ms$, while CE and our proposed VCRA (where $S = 2$) have only one RA frame composed of two RA slots.

With the aim of analyzing the performance in different condition of access load, we vary the number $K$ of devices accessing in the interval of $10ms$. We focus on a scenario with $L = 2$ access levels: the level $l = 1$ is reserved for the RA of devices

with critical charge of residual battery[5] while $l = 2$ is reserved to remaining devices. As a consequence, within the $K$ devices, a varying percentage (referred to as $\gamma$) of devices is assumed to belong the critical level.

Performance evaluation takes into consideration three parameters:

- *collision probability* $\rho$, which shows the probability for accessing devices of being forced to accomplish a novel RA due to the collision in the considered RA frame;
- *efficiency* $\eta$, which indicates how efficiently accessing resources, i.e., preambles are used. The highest the efficiency, the highest the success probability and the percentage of successful codewords compared to colliding and phantom ones.
- *overall number of decoded codewords* $N_p$, which shows the number of codewords managed by the BS during the considered RA interval. This parameters indicates the load of RAR (i.e., Msg2 of the RACH procedure) to be managed by the BS after the reception of access codewords.

For the sake of completeness, we evaluate the performance of considered schemes in different scenarios where we varied the load $\gamma = K_1/K$ of critical devices and the number of preambles (i.e., $M_1$) relevant to the related access level (i.e., $l = 1$). We consider a scenario with limited load of devices with limited battery capabilities where $\gamma = 5\%$ and 10%; in this case, we set $M_1 = 15$ (as a consequence, $M_2 = 39$). The second scenario under evaluation deals with higher loads of devices belonging to the critical access level $l = 1$ where $\gamma = 15\%$ and 20%; in this case, we set $M_1 = 20$ (as a consequence, $M_2 = 34$).

Table 3: Simulation parameters

| Parameter | Value |
|---|---|
| Number of preambles $M$ | 54 |
| Time interval | $10ms$ |
| RACH periodicity | $5ms$ |
| RA frames | 2 for 3GPP and VRA<br>1 for CE and VCRA |
| Access level | $l = 1$ High-priority<br>$l = 2$ Low-priority |
| Scenario | $M_1 = 15$, $M_2 = 39$, $\gamma = 5\%$<br>$M_1 = 15$, $M_2 = 39$, $\gamma = 10\%$<br>$M_1 = 20$, $M_2 = 34$, $\gamma = 15\%$<br>$M_1 = 20$, $M_2 = 34$, $\gamma = 20\%$ |

[5]When a device has to perform the RA, it checks the level of residual energy of its own battery. If this value is lower or equal than the energy to be spent to accomplish a number of RA procedures equal to the maximum number of allowed RA procedures, then the device belongs to high-priority access level ($l = 1$), otherwise it is assumed to be a low-priority device ($l = 2$). This reason behind this assumption is to guarantee a sufficient level of energy also to accomplish a RA procedure in the worst case, i.e., when all RA retransmissions have to be exploited by the device. Energy value can be obtained as for instance in [9].

### 5.1. Analysis of collision probability

The analysis in terms of collision probability can be found in Fig. 4.

We can easily note the strong limitations in terms of capacity of legacy-based access schemes where devices transmit only one preamble (i.e., $S = 1$). By analyzing the 3GPP RACH, the collision probability is close to 0.4 in the case of 100 devices simultaneously performing the RA procedure; it is worth noting that all devices (i.e., devices belonging to both $l = 1$ and $l = 2$ access levels) achieve the same probability of collision. As a consequence, a device with limited battery capabilities may easily occur in collisions with consequent additional battery consumptions due to the further RA procedure(s) to be performed. It is further needed to underline that the performance of 3GPP RACH does not vary in all considered scenarios. Indeed, due to the fact that all devices always exploit the same set of access preambles, the amount of high-priority devices does not influence the behavior of the RA. This aspect limits the effectiveness of 3GPP RACH as, also when the ratio of devices with low amount of residual battery is really limited compared to other ones, they may experience very high collision performance.

An interesting behavior is obtained by the VRA approach, which is able to introduce prioritization. Indeed, when observing the performance of high-priority devices (i.e., $l = 1$), we can note that VRA can effectively guarantee a lower collision probability for high-priority devices. In detail, in the case of small load of devices with critical battery ($\gamma = 5\%$), the collision probability for such devices is of about 0.067 and this is substantially lower than the one of 3GPP RACH. When $\gamma$ increases, the number of collisions increases and, in the huge case of $\gamma = 20\%$, $\rho$ becomes equal to 0.22. The side effect of prioritization in VRA scheme is the increase in the number of collisions for low-priority devices ($l = 2$). Unfortunately, this negatively impacts their performance which is poorer compared to the one achieved with 3GPP RACH. Indeed, devices belonging to $l = 2$ have a collision probability which reaches values equal to 0.5 in the heavy case of $K = 100$. These results indicates that VRA is able to effectively introduce prioritization in the RA by guaranteeing lower collision to high-priority devices at the expense of a performance degradation for other devices. This is due to the limited set of available preambles and to the use of a 3GPP-based access scheme where devices exploits only one RA slot (i.e., $S = 1$) for the RA procedure.

The CE is the best performing scheme as it achieves the lowest collision probability: this is due to the use of a RA frame composed by multiple RA slots (i.e., $S = 2$). The CE guarantees a collision probability with an order of magnitude equal to $10^{-4}$. The side effect is related to the high number of generated phantom codes which limits the effectiveness of CE approach. This will be deeply discussed in the remainder of this Section.

Our proposed VCRA approach is able to introduce prioritization similarly to VRA while also guaranteeing very low (close to CE) collision probabilities for both high- and low-priority devices. In detail, for devices with limited battery capabilities, $\rho$ varies from an order of magnitude of $10^{-3}$ (in the case of $\gamma = 5\%$) to 0.015 in the heavy case of $\gamma = 20\%$. When focusing on low-priority devices, the collision probability is almost

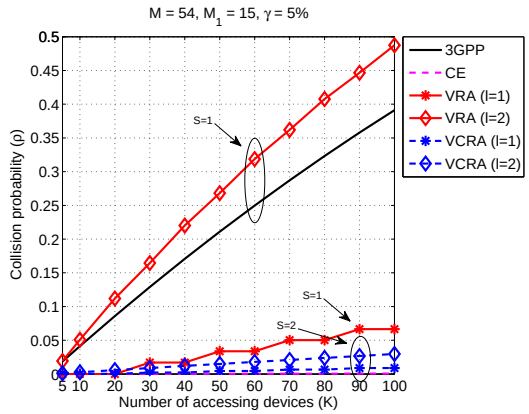


(a) $M_1 = 15,\ \gamma = 5\%$

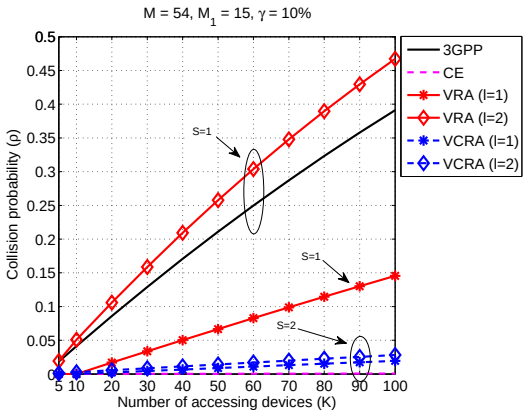


(b) $M_1 = 15,\ \gamma = 10\%$

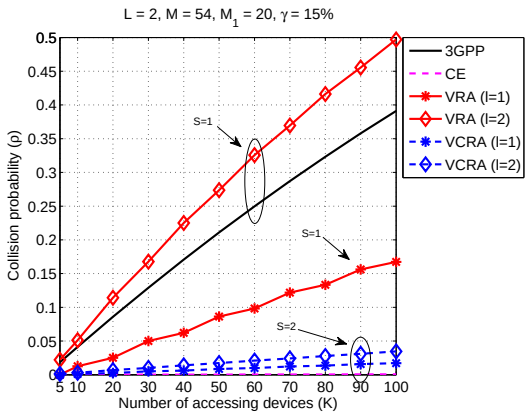


(c) $M_1 = 20,\ \gamma = 15\%$

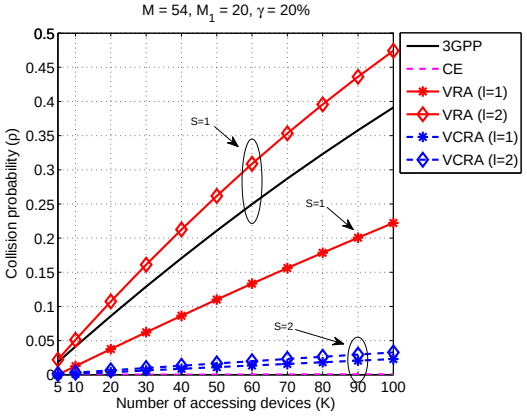


(d) $M_1 = 20,\ \gamma = 20\%$

Figure 4: Collision probability $\rho$ by varying the number of accessing devices.

equal to 0.035 in all considered scenarios; this is due to the fact that in our simulations we vary the number of preambles reserved for each access level to accommodate the varying load of high-priority devices. As a consequence, thanks to the joint exploitation of VRA and CE approaches, our proposed VCRA scheme is effective in terms of collision probability in guaranteeing prioritization without jeopardizing the performance of low-priority devices.

### 5.2. Analysis of efficiency

The analysis in terms of efficiency can be found in Fig. 5.

The achieved results testify that the VRA approach is able to guarantee high efficiency for the high-priority access level ($l = 1$). This result is related to the fact that VRA is able to offer a lower collision probability compared to 3GPP RACH and low-priority VRA and, similarly to these schemes, the VRA does not suffer in terms of phantom codes. Nevertheless, the efficiency of high-priority VRA decreases down to 0.73 when the percentage $\gamma$ of devices with critical level of residual battery increases. When focusing on low-priority VRA ($l = 2$), the efficiency is drastically lower compared to high-priority VRA and decreases down to 0.46 in the heavy case of 100 accessing devices. It is worth noting that low-priority VRA is the worst performing scheme in terms of efficiency when the number of terminals in the same access frame is higher than 80. This behavior is due to the fact that low-priority VRA has a very high collision probability.

The 3GPP RACH has an intermediate performance in terms of efficiency. When the load of terminal is limited, the 3GPP RACH outperforms the code-based approaches (except our proposed VCRA for high-priority devices) but its efficiency decreases as the load of accessing devices becomes larger. When more than 70 devices are accessing in the same access frame, the 3GPP RACH has an efficiency performance close to schemes based on the code-expanded approach.

The CE RACH has the lowest efficiency until 70 UEs, due to the fact that CE generates high number of phantom codes. It is worth underlining that the efficiency of CE does not vary meaningfully when the load of devices increases compared to other considered schemes; indeed, its performance ranges from 0.57 down to 0.51. This is due to the fact that the CE RACH is able to guarantee very low collision probability.

The performance of our proposed VCRA for low-priority terminals ($l = 2$) is almost equal to the one of CE; this is due to the fact that, although our approach has a strictly higher collision compared to CE, our VCRA approach is able to reduce the number of decoded codewords compared to CE. When considering the VCRA for high-priority devices ($l = 1$), our approach has the highest efficiency when the access load is limited (i.e., up to 10 devices), thus $\eta$ decreases. In case of low amount of critical devices ($\gamma = 5\%$), our high-priority VCRA outperforms other approaches except VRA. When $\gamma$ becomes larger, the efficiency becomes close to other 3GPP and CE schemes.

### 5.3. Analysis of decoded codewords

The analysis in terms of decoded codewords by the BS can be found in Fig. 6.

The number $N_p$ of decoded preambles for the 3GPP scheme and for VRA with $l = 2$ is in the order of magnitude of $10^2$, while it is in the order of magnitude of $10^1$ for VRA with $l = 1$.

The number $N_p$ of decoded codewords for the CE scheme and for VCRA with $l = 2$ is in the order of magnitude of $10^3$, while it is in the order of magnitude of $10^1$ for VCRA with $l = 1$.

These results testify that the high-priority access level ($l = 1$) of our proposed VCRA scheme generates a number of decoded codewords which is in the same order or magnitude of 3GPP RACH. This indicates that, although being negatively affected by phantom codes whose presence reduces the RA efficiency, our proposed VCRA does not introduce any significant increase in the number of access requests (i.e., number of received codewords/preambles) to be managed by the BS compared to the 3GPP RACH.

### 5.4. Comparison of performance results

Tab. 4 summarizes the results presented in Sec. 5.

The 3GPP RACH is characterized by an intermediate load of codewords transmitted at the base station and offers an intermediate efficiency; nevertheless, it suffers in terms very high collision probability and this aspect becomes critical when taking into account scenarios with very huge access load. Furthermore, the 3GPP RACH is not able to offer access prioritization.

The VRA scheme introduces prioritization and is able to assure a collision probability for high-priority devices lower than the one of 3GPP RACH, but still unacceptable to guarantee low latency to devices with limited battery capabilities. The price to pay is in terms of increased collision for low-priority devices, which thus experience a performance degradation compared to 3GPP RACH. In terms of efficiency, the VRA outperforms again the 3GPP RACH only when considering the high-priority access level. Finally, the load of codewords at the BS is close to the one of 3GPP RACH.

The CE approach guarantees the lowest collision probability at the expense of an intermediate efficiency (however close to that of 3GPP RACH in case of huge number of accessing devices) and of a very huge number of codewords managed by the BS.

Our proposed VCRA solution offers access prioritization where both high- and low-priority devices achieve very low collision probability (in the order of magnitude of $10^{-2}$ for both access levels). By considering the high-priority access level, our scheme is able *(i)* to guarantee very high efficiency for limited load of accessing devices and, finally, *(ii)* to keep low the number of codewords managed by the BS (almost in the same order of magnitude of 3GPP RACH). These results testify that our approach is able to introduce access differentiation without jeopardizing the RA resources for low-priority devices and without drastically increasing the number of decoded codewords at the BS for high-priority access level.

## 6. Conclusion and Future Work

We proposed a novel scheme tailored for energy-aware machine-type access on 5G smart city environments. Our ap-

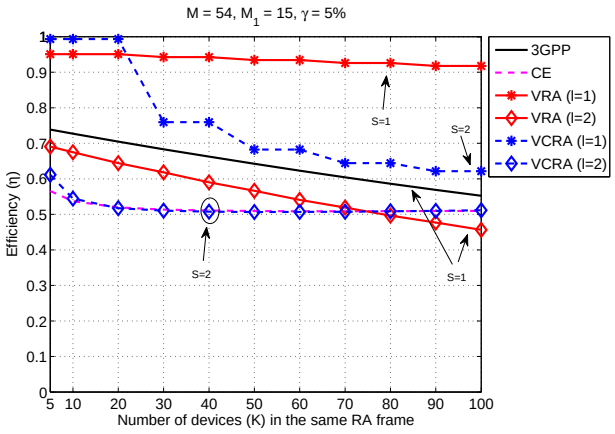


(a) $M_1 = 15,\ \gamma = 5\%$

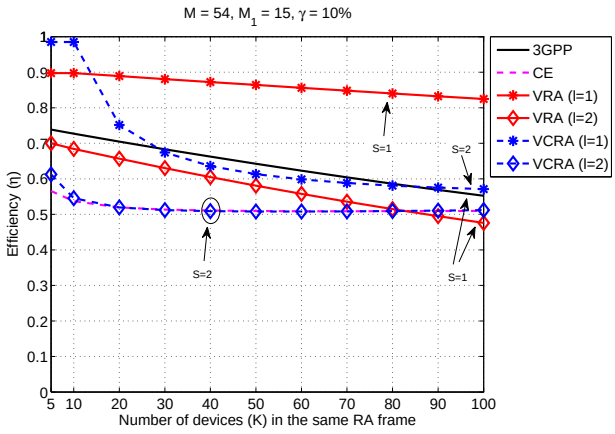


(b) $M_1 = 15,\ \gamma = 10\%$

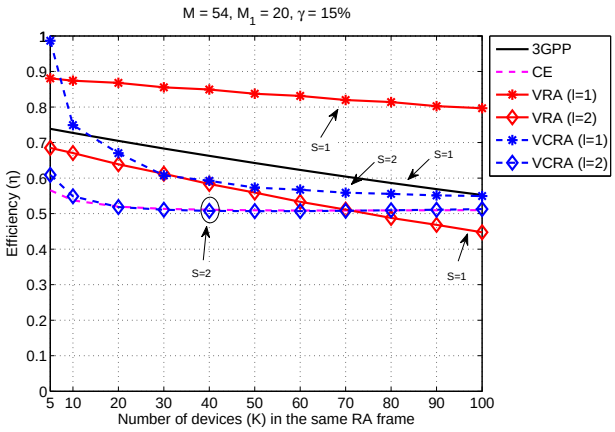


(c) $M_1 = 20,\ \gamma = 15\%$

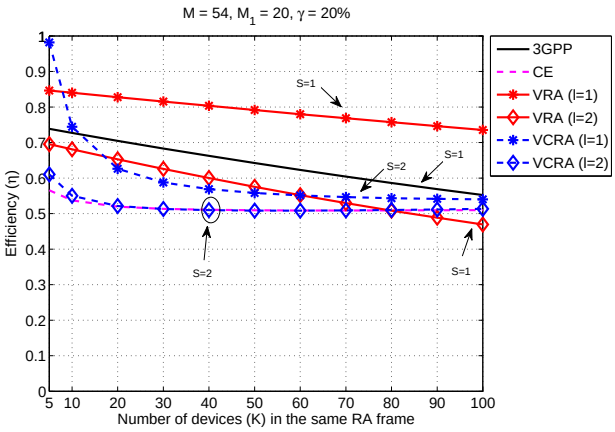


(d) $M_1 = 20,\ \gamma = 20\%$

Figure 5: Efficiency $\eta$ by varying the number of accessing devices.

Table 4: Comparison of 3GPP, VRA, CE and VCRA schemes

| | Prioritization | Collision probability | Efficiency | Number of decoded codewords |
|---|---|---|---|---|
| 3GPP | No | $\leq 0.4$ | $[0.55 - 0.75]$ | $\leq 10^2$ |
| VRA ($l = 1$) | Yes | $\leq 0.23$ | $[0.73 - 0.95]$ | $\leq 10^1$ |
| VRA ($l = 2$) | Yes | $\leq 0.5$ | $[0.45 - 0.7]$ | $\leq 10^2$ |
| CE | No | $\leq 10^{-4}$ | $[0.51 - 0.57]$ | $\leq 10^3$ |
| VCRA ($l = 1$) | Yes | $\leq 0.015$ | $[0.55 - 1]$ | $\leq 10^2$ |
| VRA ($l = 2$) | Yes | $\leq 0.035$ | $[0.51 - 0.6]$ | $\leq 10^3$ |

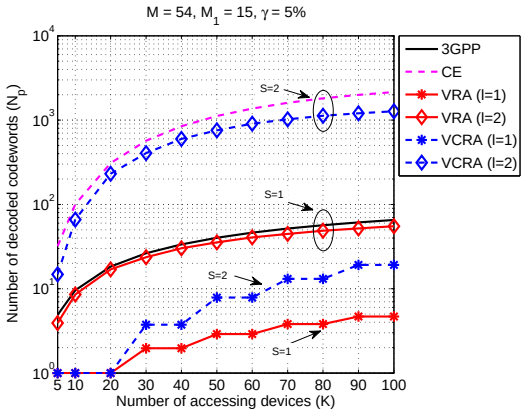


(a) $M_1 = 15,\ \gamma = 5\%$

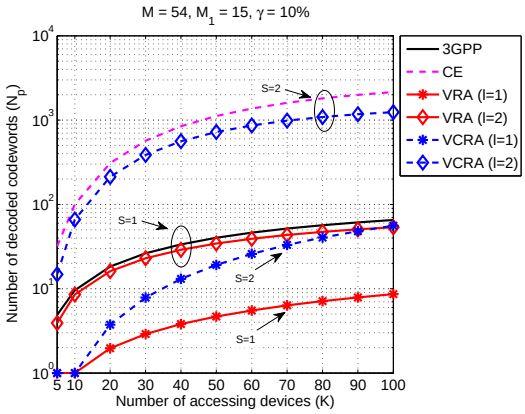


(b) $M_1 = 15,\ \gamma = 10\%$

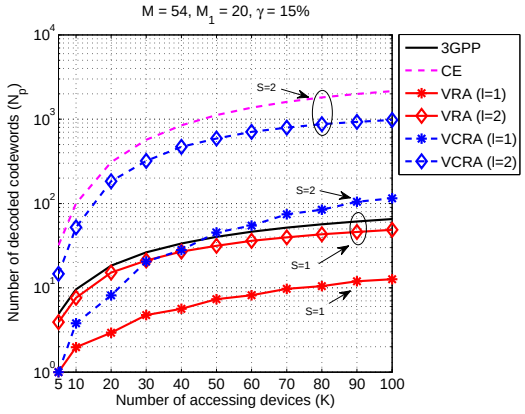


(c) $M_1 = 20,\ \gamma = 15\%$

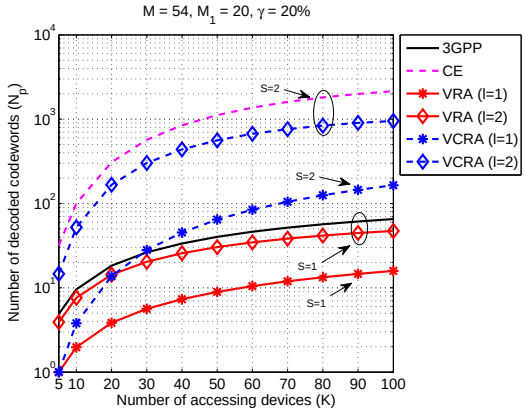


(d) $M_1 = 20,\ \gamma = 20\%$

Figure 6: Number of decoded codewords $N_p$ by varying the number of accessing devices.

proach introduces the idea of a virtual code resource allocation with the following benefits: *(i)* increase in the number of access codewords with respect to 3GPP-based access schemes thanks to the adoption of a code-expanded strategy where devices send an access codeword instead of a single one preambles; *(ii)* prioritization in the RA procedure which guarantees a lower collision probability for devices with limited battery capabilities. Simulations demonstrated the effectiveness of our approach in guaranteeing energy-differentiation among machines, supporting high load and keeping low the number of codewords to be managed by the BS.

Future work is related to the enhancements of our scheme to further reduce the impact of phantom codes.

## References


[1] C. Mulligan, M. Olsson, Architectural implications of smart city business models: an evolutionary perspective, Communications Magazine, IEEE 51 (2013) 80–85.

[2] P. Vlacheas, R. Giaffreda, V. Stavroulaki, D. Kelaidonis, V. Foteinos, G. Poulios, P. Demestichas, A. Somov, A. Biswas, K. Moessner, Enabling smart cities through a cognitive management framework for the internet of things, Communications Magazine, IEEE 51 (2013) 102–111.

[3] W. H. Chin, Z. Fan, R. Haines, Emerging technologies and research challenges for 5g wireless networks, Wireless Communications, IEEE 21 (2014) 106–112.

[4] M. Hasan, E. Hossain, D. Niyato, Random access for machine-to-machine communication in LTE-advanced networks: issues and approaches, Communications Magazine, IEEE 51 (2013) 86–93.

[5] V. Gonalves, P. Dobbelaere, Business scenarios for machine-to-machine mobile applications, in: Mobile Business and 2010 Ninth Global Mobility Roundtable (ICMB-GMR), 2010 Ninth International Conference on, pp. 394–401.

[6] M. Condoluci, M. Dohler, G. Araniti, A. Molinaro, K. Zheng, Toward 5g densenets: architectural advances for effective machine-type communications over femtocells, Communications Magazine, IEEE 53 (2015) 134–141.

[7] K. Zheng, S. Ou, J. Alonso-Zarate, M. Dohler, F. Liu, H. Zhu, Challenges of massive access in highly dense lte-advanced networks with machine-to-machine communications, Wireless Communications, IEEE 21 (2014) 12–18.

[8] K. Zheng, S. Ou, J. Alonso-Zarate, M. Dohler, F. Liu, H. Zhu, Challenges of massive access in highly dense LTE-advanced networks with machine-to-machine communications, Wireless Communications, IEEE 21 (2014) 12–18.

[9] A. Laya, L. Alonso, J. Alonso-Zarate, Is the random access channel of lte and lte-a suitable for m2m communications? a survey of alternatives, Communications Surveys Tutorials, IEEE 16 (2014) 4–16.

[10] More than 50 billion connected devices, White Paper, 2011.

[11] K. Zheng, F. Hu, W. Wang, W. Xiang, M. Dohler, Radio resource allocation in LTE-advanced cellular networks with M2M communications, Communications Magazine, IEEE 50 (2012) 184–192.

[12] 3GPP, RAN Improvements for Machine-type Communications, Technical Report TR 38.868, 2011.

[13] J.-P. Cheng, C. han Lee, T.-M. Lin, Prioritized Random Access with dynamic access barring for RAN overload in 3GPP LTE-A networks, in: GLOBECOM Workshops (GC Wkshps), 2011 IEEE, pp. 368–372.

[14] H. Thomsen, N. K. Pratas, C. Stefanovic, P. Popovski, Code-expanded radio access protocol for machine-to-machine communications, Transactions on Emerging Telecommunications Technologies 24 (2013) 355–365.

[15] 3GPP, Study on RAN Improvements for Machine-Type Communications, Technical Report TR 37.868, 2011.

[16] 3GPP, Evolved Universal Terrestrial Radio Access (E-UTRA); Radio Resource Control (RRC), Technical Report TS 36.331, 2012.

[17] C. Mehlfuhrer, M. Wrulich, J. Ikuno, D. Bosanska, M. Rupp, Simulating the Long Term Evolution physical layer, in: Signal Processing Conference, 2009 17th European, pp. 1471–1478.